Theory of Gamma-Ray Loud AGNs

Frank M. Rieger[a,b]

[a] *Institute for Theoretical Physics, Heidelberg University, Philosophenweg 12, 69120 Heidelberg, Germany*
[b] *Max-Planck-Institute for Nuclear Physics (MPIK), P.O. Box 103980, 69029 Heidelberg, Germany*

E-mail: f.rieger@uni-heidelberg.de

The last decade has seen tremendous developments in gamma-ray astronomy with the extragalactic sky becoming highly populated by Active Galactic Nuclei (AGNs). This brief review highlights some of the progress in AGN research achieved over the years, and discusses exemplary advances in the theory and physics of gamma-ray loud AGNs, including black-hole magnetospheric processes, the physics of pc-scales jets, as well as particle acceleration and high-energy emission in the large-scale jets of AGNs.

1. Introduction

Radio-loud or *jetted AGNs* [1], i.e. AGNs with strong relativistic jets, are the most persistent, powerful sources in the Universe. Their detection at gamma-ray energies reveals that a significant amount of their power is deposited a highest energies, and demonstrates them to be exceptional cosmic particle accelerators [2]. All types of jetted AGNs have been seen at gamma-ray energies, from more misaligned radio galaxies to blazar-type sources where the jets are seen face-on [3–5]. Gamma-ray astrophysics is thus expected to play a fundamental role in resolving key issues in AGN physics, such as: *(i) How are relativistic jets being formed?* Are they preferentially ergospheric or disk-driven? If the former, what is their plasma source; if the latter, what is their accretion-disk connection? *(ii) What makes jets radiate?* What is the dominant gamma-ray radiation process and particle acceleration mechanism? Where is it located? What is the plasma composition? *(iii) How are small and large scales connected?* How is the energy transported from the black hole (BH) to the outer lobes scales? How are jets confined? What kind of instabilities are important?

2. On the Extragalactic Gamma-Ray Sky

The extragalactic sky has become bright at gamma-ray energies. The Fermi-LAT 12 year point source catalog (4FGL-DR3) for example, reports the detection of 6658 sources at high energies (HE) > 50 MeV, with more than 3740 identified as belonging to the blazar class of AGNs, cf. Fig. 1. About 70 sources have been identified as non-blazar AGNs, out of which 45 are radio galaxies
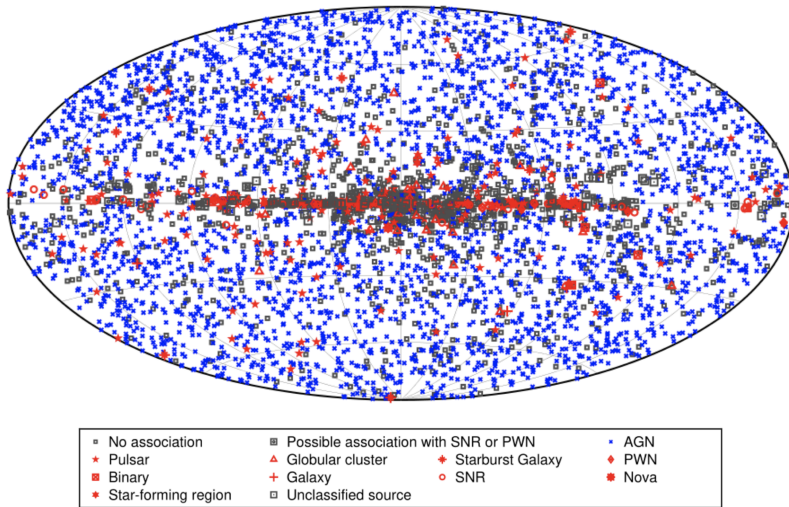

Figure 1: High-energy sky map (4FGL) based on 8 yr of Fermi-LAT data. All AGNs (all classes) are plotted with the same blue symbol. From ref. [6]. ©AAS. Reproduced with permission.

(among them 22 Fanaroff-Riley (FR) I and 14 FR II) and 8 are Narrow Line Seyfert 1 (NLSy 1) galaxies [6, 7]. At very high energies (VHE; ≥ 100 GeV), about 85 AGNs are listed in the TeVCat catalog, with redshifts up to $z \simeq 1$. While most of the TeV sources are BL Lac objects (55 HBL, 10 IBL, 2 LBL), a few prominent radio galaxies (e.g., Cen A, M87 and NGC 1275) are present as well. The latter sources have raised considerable interest by allowing insights into the immediate vicinity of the supermassive BH environment in AGNs (cf. Sec. 4.1 below). For a recent review of

the physics case of gamma-ray emitting, non-blazar AGNs, the reader is referred to ref. [8]. Spectral and timing capabilities at gamma-ray energies have significantly developed over time, allowing, in some sources, to probe rapid variability down to a few minutes and unusual spectral features that could signal new physical processes, see e.g., Fig. 2.
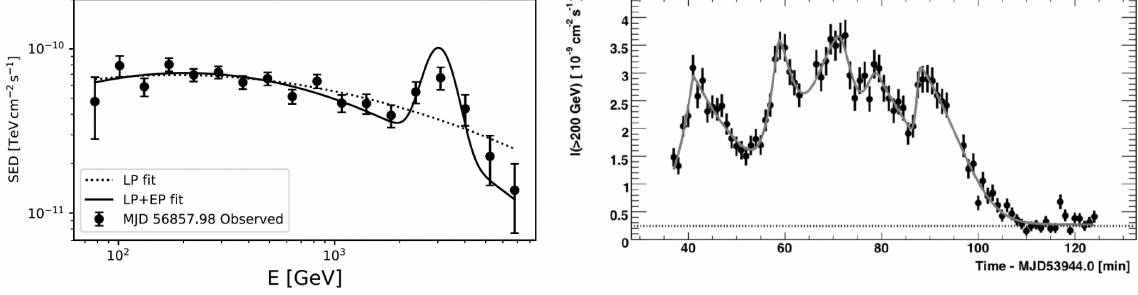

Figure 2: *Left:* The VHE SED of Mkn 501 ($z = 0.034$) during an elevated state in 2014 July 19 as measured by MAGIC, revealing an unusual feature at $\sim$ 3 TeV. From ref. [9], reproduced with permission © ESO. *Right:* The VHE light curve of PKS 2155-304 ($z = 0.116$) during its famous outburst in July 2006 as seen by H.E.S.S., revealing substantial flux changes down to $\sim$ 3 min. From ref. [10].

The detection of NLSy 1 galaxies at HE energies has raised several issues. Radio-quiet (non-jetted) NLSy 1 are commonly thought to be high-Eddington sources, with moderate BH masses ($\sim 10^{6-8} M_\odot$), which are hosted by spiral galaxies [11]. Since HE-emitting (radio-loud) NLSy 1 appear to be of the jetted AGN type, showing some blazar-like properties such as one-sided jets and superluminal motion, this has triggered discussion about the BH mass limit and accretion/merger history conducive for the origin and formation of relativistic jets. Relevant to this discussion is the question, whether jetted NLSy 1 might belong to a special subclass harbouring BHs with larger masses and hosted by elliptical galaxies instead. There are growing indications, however, that many of them are better modelled as disk-like galaxies [12]. For a discussion of these topics and related literature, the reader is referred to the recent overviews in refs. [13, 14].

3. On Challenges and Progress in (jetted) AGN Physics

3.1 Challenges in AGN Physics

Understanding the physics of AGN jets and the role played by its supermassive BH is a challenging, multi-scale problem. Phenomenologically, the *observed scale separation* covers a range of almost ten orders (as in, e.g., Cen A) of magnitude, see e.g. Fig. 3. This fact translates into a fundamental *physics and modelling challenge* of how to consistently bridge these different scales, e.g., of how to connect the global, source dynamical scale, the radiation (e.g., synchrotron, inverse Compton) scale and the dissipation (e.g., shock, reconnection, turbulence) scale. While solid progress has been achieved over the years, no complete picture is existing up to now. In principle, this also applies to numerical simulations (cf. [16, 17] for related reviews). While essential to inform and advance our understanding, they are not without caveats, i.e., in general, AGN physics is also accompanied by a *methodological (computational) challenge*. In the context of jet formation for example, conventionally employed *general-relativistic/magneto-hydrodynamic*
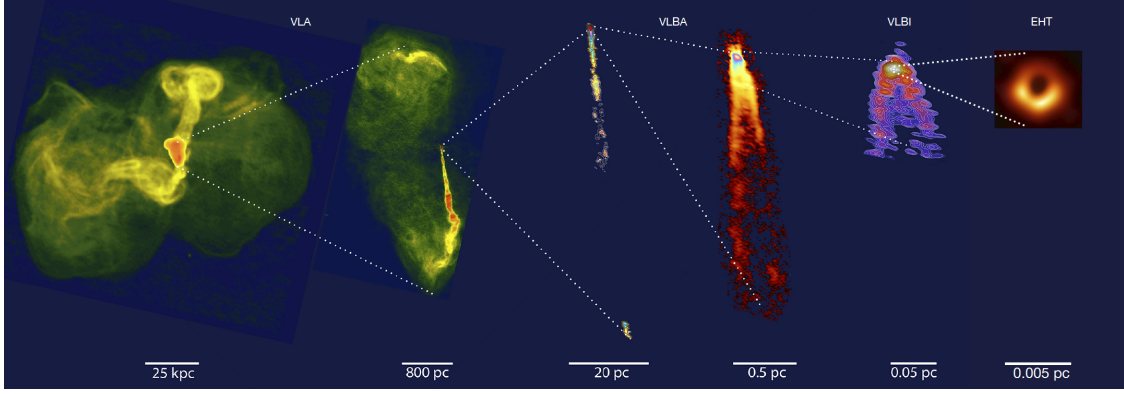
Figure 3: The radio galaxy M87 as seen from large, radio-halo (VLA) down to black-hole (EHT) scales, corresponding to an "observed scale separation" of $\sim 10^8$. Adapted based on ref. [15].

(GR/MHD) simulations usually rely on an ambiguous numerical floor model; methodologically, it may seem rather surprising that a single fluid description is able to provide important insights (as it has) in cases where we expect the plasma to be collisionless; further, in ideal MHD there is little physical understanding of reconnection, particle acceleration and radiation, and so forth. On the other hand, first-principle *particle-in-cell (PIC)* simulations in astrophysics mostly deal with highly idealized setups, often in reduced dimensionality and for quite limited duration, along with artificially large gyro-radii. In fact, in the case of AGNs, the relevant scale separation (system size r vs plasma skin depth l_p) can be as high as $r/l_p \sim 10^{6-8}$, cf. ref. [18], and it remains unclear to which extent features seen in these simulations might persist up to the physical scale of interest. Notwithstanding these limitations, numerical simulations have become an indispensable tool for progress.

3.2 Progress in AGN Physics

The last years have seen both, significant progress and consolidation of knowledge in our understanding of the physics of AGNs. The following provides a short selection of exemplary results with relevance to gamma-ray emitting AGNs.[1]

3.2.1 Supermassive Black Holes in the Center of AGNs

The presence of supermassive BHs in galactic nuclei has been suggested for more than half a century based on strong theoretical arguments. Early experimental efforts related to dynamical searches have been described ~ 25 yr ago [19]. Most recently, theoretical and experimental progress in BH research has eventually been documented by the 2020 Nobel prize for Physics to Roger Penrose, Reinhard Genzel and Andrea Ghez. While the benchmark BH Sgr A* is not (yet) an established gamma-ray emitter [20], the event horizon telescope (EHT) radio image of the BH shadow in M87 [21] provides important information relevant to VHE research. The size $\simeq 2.5r_s$ of the photon ring in M87 (where $r_s := 2r_g := 2GM_{BH}/c^2$), implies a BH mass of $M_{BH} \simeq 6.5 \times 10^9 M_\odot$ and constrains horizon scale (minimum) variability to $t_H \simeq 0.38$ d, close to what can be probed

---

[1]For recent results on hadronic processes and neutrino emission, the reader is referred to the related reviews by Paolo Padovani and Elisa Resconi.

with VHE instruments [8]. Further research along these lines (by, e.g., the next-generation EHT) will allow to probe deeper into the central engine in AGNs (BH - disk - jet, its connection and dynamics), and tighten the constraints on the current jet power (e.g., BH spin) relevant to VHE emission models.

3.2.2 Convergence of theoretical, numerical & observational evidence for jet stratification

There is consolidation of knowledge that the jets in AGN are multi-layered, revealing a lateral stratification similar to the one induced by a fast BH-driven (Blandford-Znajek: BZ, [22]) jet surrounded (and possibly confined) by a slower moving disk-driven outflow, cf. [23]. Resolved (lateral) emission structures such as limb-brightening and linear polarisation signatures, e.g., refs. [24, 25], substantiate early two-flow and spine-sheath type non-thermal emission models [26, 27]. In the case of M87, for example, significant structural patterns across the jet on sub-pc-scale have been detected, indicating the presence of both slow ($\sim 0.5c$) and fast ($\sim 0.92c$) components [28]. Pronounced edge-brightened features have now been seen in both, M87 and Cen A [29]. In the high energy context, characterising internal jet stratification is potentially important to, e.g., address the (putative) Doppler factor "crisis" in TeV (HBL) blazars [30], to develop more advanced acceleration (cf. Sec. 4.3) and emission models, and to probe into AGN unification scenarios (e.g., relative power of inner vs outer jet?).

3.2.3 Acceleration and collimation of relativistic jets

Detailed radio studies now provide insights into the jet collimation profile in more and more nearby sources [31, 32]. In the case of M87 for example, the jet width profile is initially (semi-)parabolic and then transitions (at around the Bondi radius $r_B \sim 5 \times 10^5 r_g \sim 150$ pc) to a conical shape, see Fig. 4. There is evidence that the radio flow is initially slow (on scales ~ 0.03 pc) and gradually accelerates with distance, reaching $\Gamma\beta \sim 3$ on scales of r_B [33, 34]. This can be
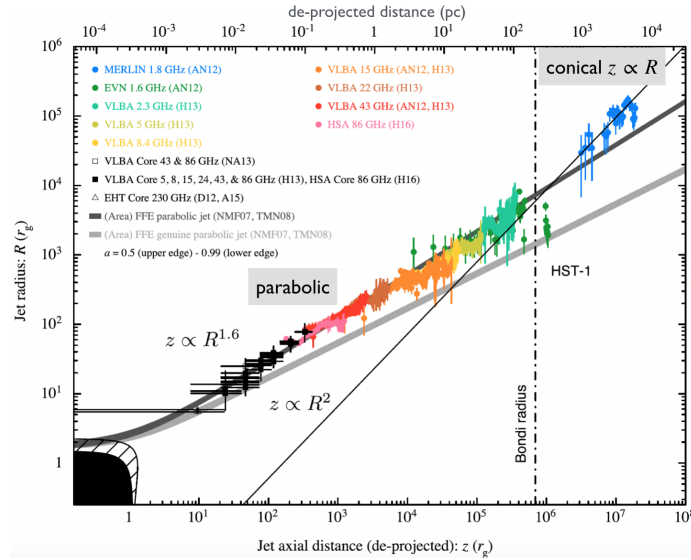

Figure 4: The jet collimation profile for the radio galaxy M87 from sub-parsec to kilo-parsec scales. From ref. [33]. ©AAS. Reproduced with permission.

understood in terms of a jet that is magnetically dominated at its base and whose magnetic energy is gradually converted into kinetic energy while experiencing some external confinement [35, 36]. These results are instructive for improving our understanding of the non-thermal emission in low-luminosity FR I type sources, and of the dynamical role (confinement) played by a disk-driven wind. While consequences of flow deceleration on high-energy SED modelling have been explored in the past [37], consideration of flow acceleration seems an important desideratum.

3.2.4 Convergent evidence for relativistic motion in large-scale AGN jets

While jets experience deceleration on larger scales, they can still be substantially relativistic on kilo-parsec scales, even for moderately powerful sources. The nearby ($d \sim 95$ Mpc) FR I radio galaxy 3C 264 is a prototype example (with estimated jet power $L_j \sim 5 \times 10^{43}$ erg/s) [38], exhibiting superluminal motion and collision of knots (internal shocks) in HST observations on scales of $\sim (0.5 - 1)$ kpc, corresponding to a bulk flow Lorentz factor $\Gamma \sim 7$ and a Doppler factor $D \sim 7$ for an inclination $\theta \sim 8°$ [39]. These findings are of interest not only because 3C264 is a recently detected VHE emitter [40], but also by offering general insights into particle acceleration at shocks, and the role of nearby large-scale jets as putative sites of ultra-high energy cosmic ray (UHECR) acceleration.

3.2.5 Extreme TeV blazars

A sizeable fraction of VHE-emitting AGNs ($\sim 1/4$ of all HBL) are now composed of BL Lac objects with hard intrinsic VHE spectra, i.e. with de-absorbed power-law (PL) photon indices $\Gamma_{\text{VHE}} \lesssim 1.5 - 1.9$, implying an SED bump peaking above 1 TeV, see ref. [4] for a review. The prototypical source of these extreme highly peaked BL Lacs (EHBLs) is 1ES 0229+200 ($z = 0.14$) with an SED peak (de-absorbed) above 4 TeV. The SED modelling of these sources is challenging, and in the common synchrotron-self Compton (SSC) approach requires unusual (if not extreme) conditions such as an electron distribution with a very high minimum Lorentz factor $\gamma_{\text{min}} \gtrsim 10^4$, or one following a relativistic Maxwellian [41]. The narrow pile-up feature seen in Mkn 501 [9], cf. Fig. 1 (left), might be reminiscent of the latter [42]. These extreme TeV blazars are particularly interesting as they indicate emitting regions significantly away from equipartition ($u_B/u_e \lesssim 10^{-4}$ in SSC). The implied low magnetisation σ would seem to disfavour reconnection and instead point to stochastic or multiple shocks as possible acceleration mechanism (see also Sec. 4.2). VHE variability studies will enable to probe into this as only modest ($\geq$ month-type) intrinsic variability would be expected (unless geometrical effects would interfere). Unusual spectral shapes at VHE energies will complicate EBL (Extragalactic background light) studies using simple extrapolation functions (for a recent review of developments, see e.g. ref. [43]).

3.2.6 Gamma-Ray Astrophysics in the Time Domain

Within the last decade, gamma-ray astronomy has successfully entered the time domain [44]. Key examples include the detection and characterisation of ultra-fast VHE variability (down to a few minutes) [4, 45] as well as evidence for year-type quasi-periodic oscillations (QPOs) in the Fermi-LAT light curves of blazars [46, 47]. A prominent example of the latter is the HBL object PG 1553+113 ($z \sim 0.5$) with an (observed) HE period of $\simeq 2.2$ yr, possibly caused by a close supermassive binary BH system (SBBHs) [48, 49]. Application of more advanced time series

techniques, exploring power-law noise characteristics and log-normality has been steadily growing [50]. Theoretical efforts are now gaining momentum, cf. [44] for a review, and refs. [51, 52] for selected contributions. Properly understanding the variability characteristics has important implications for the origin of the emission (e.g., location and driving process) and the overall source dynamics and evolution (e.g., SBBHs, disk physics).

4. Selected Theoretical Advances

The following subsections aim to provide exemplary and more detailed insights into three different fields where theoretical advances in AGN physics, whether conceptual or methodological, have been significantly influenced by gamma-ray observations.

4.1 Magnetospheric Processes in AGNs

The detection of VHE variability on BH horizon crossing time scales ($\sim r_g/c$), as in e.g. M87, has been a significant driving force for the development of magnetospheric particle acceleration and emission models, see e.g. ref. [8] for a review. Magnetic fields that are brought in and dragged into rotation (Ω_F) by the BH can induce an electric field component (parallel to the magnetic field), that, if not screened, can facilitate efficient particle acceleration. This could potentially occur either around the so-called null surface across which the Goldreich-Julian [53] charge density, $\rho_{GJ} \sim (\Omega_F - \omega)B$, required to screen the electric field, changes sign, or at the stagnation surface that separates MHD in- and outflows, see Figure 5. The maximum available voltage drop for a BH
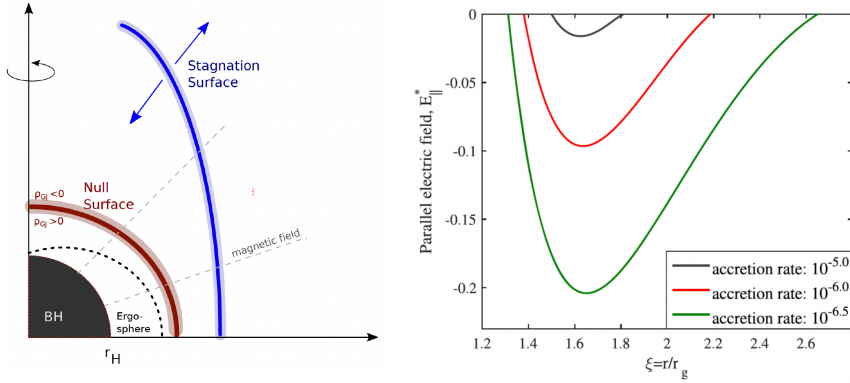

Figure 5: *Left:* Illustration of possible locations of charge-deficient regions (gaps) around a rotating BH. The red line denotes the null surface across which ρ_{GJ} changes sign, while the blue line delineates the stagnation surface from which stationary MHD flows start. *Right:* Exemplary gap evolution for a Kerr BH of $10^9 M_\odot$ accreting in a radiatively inefficient mode. The curves show the radial distribution of the parallel electric field around the null surface for different accretion rates $\dot{m}$. The gap width and voltage drop increase as $\dot{m}$ drops because pair creation of energetic photons with the soft photon field becomes less efficient. From ref. [54].

gap of width h is of the order of [55]

$$\Delta\Phi = \frac{1}{c}\Omega_F r_H^2 B_H (h/r_g)^2 \simeq 2 \times 10^{21} \dot{m}^{1/2} M_9^{1/2} (h/r_g)^2 \, [V], \tag{1}$$

for a horizon-threading field $B_H \simeq 2 \times 10^5 \dot{m}^{1/2} M_9^{-1/2}$ G, where $M_9 \equiv M_{BH}/10^9 M_\odot$, $\Omega_F = \Omega_H/2 = c/4r_g$, and $\dot{m} \equiv \dot{M}/\dot{M}_{Edd}$. Electrons that get accelerated in these gaps produce γ-rays

7

via curvature radiation and inverse Compton (IC) up-scattering of ambient soft photons, producing an observable and variable VHE signal [56]. Interaction ($\gamma\gamma$-absorption) of energetic γ-rays with low-energy soft photons can trigger a pair cascade that generates plasma and ensures closure of the gap [8]. On conceptual grounds, magnetospheric gaps thus provide a self-consistent means for the continuous plasma supply ("numerical floor") needed to activate a force-free (BZ) MHD outflow [57]. Correspondingly, unless accretion rates are sufficiently low (i.e., well below $\dot{m} \sim 10^{-4}$), efficient pair production will occur (if non-negligible gaps form at all, cf. [56, 58]), leading to gap sizes $h \ll r_g$, thereby significantly reducing the accessible gap potential, cf. eq. [1]. Typically, achievable (radiation-limited) electron Lorentz factors are constrained to $\gamma_e \sim 10^{8-10}$ [55]. To improve insights into characteristic electric field strengths and achievable voltage drops, one can seek for self-consistent steady gap solutions [54, 58] by solving the system of relevant partial differential equations (e.g., Gauss' law, equation of particle motion, continuity equation), see e.g. Figure 5 (right). For example, taking an accretion rate $\dot{m} = 10^{-5.75}$, which is close to the mean MAD value used in EHT-GRMHD simulations for M87 [59] and which corresponds to jet powers of a few times 10^{43} erg/s, the gap properties for M87 (assuming the inner disk to be ADAF-type) can be evaluated [54]. The resultant gap sizes are of the order of $\sim 0.8 r_g$, suggesting that the VHE emission in M87 might be variable down to timescales of ~ 0.4 days. The inferred gap power of $\sim 5 \times 10^{41}$ erg/s would make it in principle possible to accommodate the VHE emission seen during its high states [60]. The achievable voltage drop would be of the order of $\sim 10^{18}$ V, suggesting that the BH in M87 is not an efficient UHECR proton accelerator. The appreciation that gap operation is expected to be intermittent, has in recent times triggered a variety of time-dependent investigations using PIC simulations, see e.g. refs. [61–64]. Relative comparison is often not straightforward as different setups and complexities have been employed (e.g., with regard to box sizes, cell numbers, run times, 1d/2d, radiation reaction, choice of soft photon field). Generically, the outcome is highly sensitive to the assumed ambient soft photon field (i.e., minimum photon energy $\epsilon_{\min}$ and spectral shape, e.g., PL index), making an adequate description an important prerequisite as it determines the efficiency of pair cascades. There are indications for a periodic opening (timescale $\sim r_g/c$) of macroscopic gaps (with $h \sim [0.1-1] r_g$), cf. Fig. 6. Issues that deserve further studies concern e.g., the degree to which detected oscillation periods could be dependent on the simulation setup (e.g., box size), and the extent to which the emerging particle distributions might be bimodal. Insights gained will help to better characterise the link between gap activity, VHE flaring and jet formation.

4.2 Modelling Parsec-Scale Jet Emission in Blazars

The spectral energy distributions (SEDs) of gamma-ray blazars have for long been modelled by leptonic (SSC) and/or hadronic (e.g., $p\gamma$) radiation processes, see e.g. [65, 66] for a review. Quite often their SEDs can be satisfactorily reproduced with different sets of assumptions, which significantly limits inferences on the source physics. Incorporating microphysical insights from kinetic plasma simulations into SED modelling can allow an important step forward. One exemplary context relates to the requirement of high minimum electron Lorentz factor $\gamma_{\min,e}$ and low magnetisation σ in SSC models for extreme TeV blazars (cf. Sec. 3.2.5). A recently proposed framework considers co-acceleration (diffusive shock) of electrons and protons at mildly relativistic (e.g., $\Gamma_s \sim 3$), weakly magnetised (internal or recollimation) shocks in blazar jets [67]. Shocks are known to convert a significant fraction of the kinetic energy of the incoming plasma flow to thermal
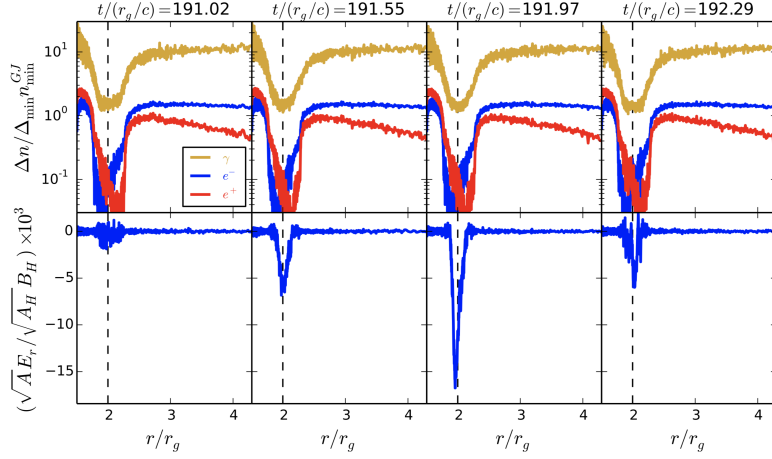
Figure 6: Exemplary gap cycle seen in 1d PIC simulations (spit monopole field) for a steep ambient photon field (n_s) with $\epsilon_{min} = 0.0005$ eV and fiducial Thomson depth $\tau_0 := n_s \sigma_{Th} r_g = 100$ (yielding a pair creation length $\sim 0.3 r_g$). Top panel: Evolution of the normalized densities of electrons, positrons and photons. Bottom panel: Evolution of the electric field. Vertical dashed line denotes the null surface. From ref. [63]. ©AAS. Reproduced with permission.

energy, represented by a Maxwellian particle distribution $n(\gamma) \propto \gamma^2 \exp[-\gamma/\Theta]$ with $\Theta \equiv k_B T/mc^2$. Assuming an efficient energy transfer (heating/thermal coupling) from protons to electrons in the shock transition layer, one can write $k_B T_P \sim \Gamma_s m_p c^2$ and $T_e = \xi T_p$ where $\xi < 1$, with Γ_s the Lorentz factor of the shock. If the peak in the Maxwellian electron distribution is identified with $\gamma_{min,e}$, then roughly $\gamma_{min,e} \sim k_B T_e/(m_e c^2)$, i.e.

$$\gamma_{min,e} \sim \left(\frac{m_p}{m_e} \right) \Gamma_s \xi \simeq 1800 \, \Gamma_s \xi \qquad (2)$$

Hence, given suitable conditions, a high $\gamma_{min,e}$ is naturally expected. In PIC simulations of highly relativistic shocks, efficient Fermi-type particle acceleration has only been seen for weakly magnetized (e.g., $\sigma \lesssim 10^{-3}$) shocks, in line with considerations in the above framework. Since these shocks will also generate magnetic (micro)turbulence, the effective magnetization ($\sigma := B^2/(4\pi\langle\gamma\rangle nmc^2$) could in principle be higher than the pre-shock one, yet decaying downstream with distance. Accordingly, the magnetization in the radiation zone, σ_{rad}, may be in the range $\sigma \lesssim \sigma_{rad} \lesssim 0.01$.

For high (Alfvenic) Mach numbers, significant thermal coupling can occur. In large 2d PIC simulations of quasi-parallel, mildly relativistic ($\beta_s \simeq 0.8$), weakly magnetized ($\sigma = 0.007$, defined downstream) electron-ion shocks (with reduced mass ration $m_p/m_e = 64$), for example, $T_e \sim (0.2-0.3) T_p$ and $k_B T_p \sim 0.2 m_p c^2$ has been seen, cf. Fig. 7 [68]. For smaller magnetizations and larger shock speeds, electron preheating can be further increased [69, 70]. Figure 8 shows an exemplary reproduction of the SED of the prototypical EHBL 1ES 0229+200 motivated by such a framework. In this case, re-acceleration at multiple ($n \geq 2$) shocks is needed to account for the hard particle spectra required for spectral fitting. This leads to a modification (hardening and power-law deviation) of the input, single shock electron spectrum (of power law momentum index $s = 2.2$), and also increases the effective injection Lorentz factor to $\gamma_{min,eff} \sim \Gamma_s^{2n/3} \gamma_{min,e}$ [67]. The noted framework represents an exemplary approach to utilise microphysical insights for blazar
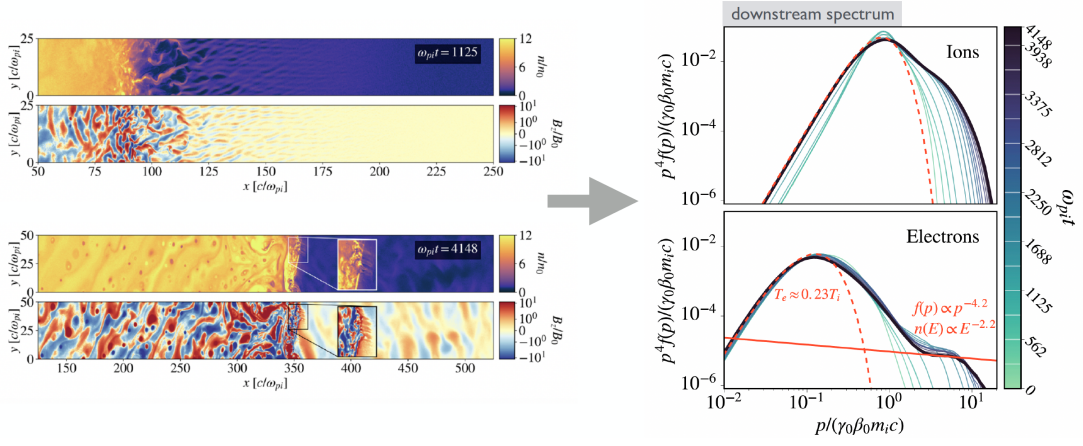
Figure 7: 2d PIC simulations of a weakly magnetized, mildly relativistic, high Mach number ($M_A = 15$) shock with $\Gamma_s \simeq 1.7$. *Right:* Shock evolution and magnetic field generation (initially Weibel-, later Bell-mediated) with time. *Right:* Downstream particle distributions $p^4 f(p)$ at different times, with the formation of a non-thermal power-law tail on top of a thermalized particle distribution. At late times, the downstream electron temperature is $20 - 30\%$ of the ion temperature, indicating significant coupling. Based on ref. [68].
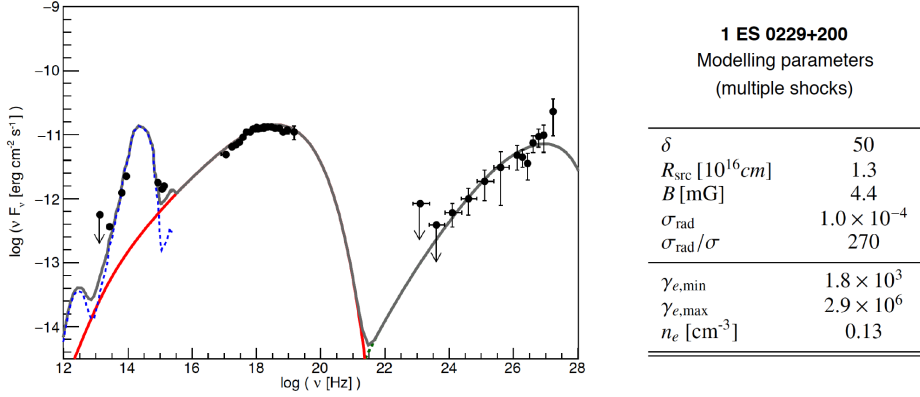

Figure 8: Reproduction of the SED of the EHBL source 1ES 0229+200 in a multiple shock scenario with input parameters for the initial electron distribution as shown in the table to the right. From ref. [67], reproduced with permission © ESO.

SED modelling. One central assumption is that the emission arises in a jet region that is kinetically dominated by an electron-proton composition (with protonic emission expected to be suppressed) rather than an e^+e^- one. Similar indications have been found in the case of another prominent γ-ray blazar, PKS 2155-304, based on a statistical analysis of its X-ray emission [71], though there is also other evidence (based on optical circular polarization) suggesting that the (non-thermal) positron fraction cannot be too low [72], cf. also ref. [73]. A possible caveat for the noted approach relates to the model requirement of a region significantly out of equipartition and characterized by a very low magnetic field. In principle, variability studies could allow to probe into these assumptions.

A related framework considers the electrons in the jet to be (initially) diffusively accelerated at a recollimation-type shock, but then further energized through stochastic (2nd order Fermi) acceleration in the downstream flow [74]. Hence, instead of acceleration at multiple shocks, recollimation

in a weakly magnetized flow is presumed to result in strong turbulence. While the synchrotron spectrum can be satisfactorily reproduced in a SSC model where synchrotron cooling is comparable to particle escape (cf. also [41] for another variant), the Compton SED component appears somewhat too hard. Since EHBL SED models are in general far from equipartition (i.e., $\sigma \ll 1$), characteristic Alfven speeds are sub-relativistic ($v_A \propto \sqrt{\sigma} \ll c$) making stochastic acceleration less efficient ($t \propto 1/v_A^2$), so that it remains to be explored to what extent a self-consistent SED fit can be achieved. Nevertheless, these approaches represent instructive examples of how to fruitfully combine insights from jet simulation, particle acceleration physics and SED modelling.

4.3 Understanding the large-scale jet emission of AGNs

The origin of extended X-ray emission along the large-scale jets in AGNs has for long been a matter of debate, with electron-synchrotron and IC-CMB scenarios as the leading contenders, see e.g. [75, 76] for review. Within more recent years, however, IC-CMB models have been disfavoured in an increasing number of sources as they tend to, e.g., over-predict Fermi-LAT gamma-ray flux limits [77, 78] or are not supported by detailed X-ray spectral information [79]. An electron synchrotron origin, however, requires to maintain electrons with Lorentz factors $\gamma_e \sim 10^8$ all along the jet. The short cooling timescales $t_{\rm cool} \propto 1/\gamma$ of these electrons, and correspondingly short cooling lengths $ct_{\rm cool} \ll 1$ kpc, calls for the operation of a "distributed" acceleration mechanism along the jet, beyond "localised" shock acceleration. The recent detection of extended VHE emission along the kpc-scale jet of Cen A [80] has provided an important validation to this picture, see Fig. 9, by directly tracing the electrons and removing the degeneracy (B, γ) inherent in an X-ray synchrotron model. IC up-scattering of dust by ultra-relativistic (synchrotron X-ray emitting) electrons with $\gamma_e = 10^8$ accounts for the observed VHE emission and confirms the X-ray synchrotron interpretation. The results imply a jet that is only weakly magnetized ($\sigma < 0.5$) on kiloparsec scales. Stochastic (2nd order Fermi) and shear particle acceleration processes are among the most promising
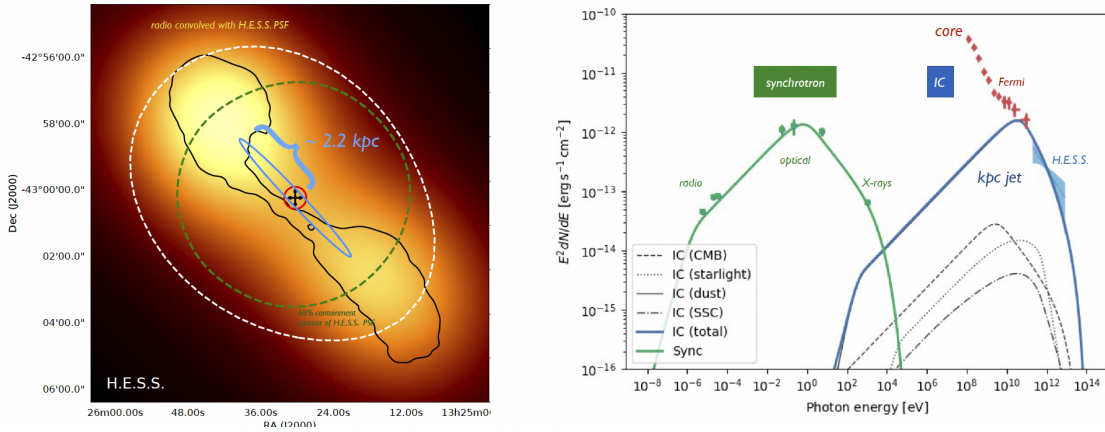

Figure 9: Extended VHE emission along the kpc-scale jet of Cen A as seen by H.E.S.S. The SED of the kpc-scale jet can be reproduced by means of an (exponential-cutoff) broken-power law electron distribution with $\gamma_b \simeq 10^6$ and cut-off energy $\gamma_c \simeq 10^8$, for a characteristic jet magnetic field strength of $B \simeq 20\mu G$. Interestingly, IC emission by the kpc-scale jet may be behind the unusual spectral hardening [81] seen at GeV energies. Based on ref. [80].

mechanisms facilitating continuous re-acceleration in kinetically dominated jets [82–85]. Particle

acceleration in the latter framework essentially draws on the jet flow velocity difference that a charged particles experiences as it moves across the jet shear (cf. Sec. 3.2.2), see e.g. ref. [86] for an accessible introduction. It can be viewed as a second-order ($\Delta E \propto u_{\rm sc}^2 E$) Fermi-type acceleration process, in which the common scattering center speed, $u_{\rm sc}$, is replaced by an effective velocity, $\bar{u}$, determined by the shear flow profile, i.e., by the characteristic flow velocity change sampled over the mean free path $\lambda \simeq \tau c$ of the particle. Hence, for instance $\bar{u} = (\partial u_z/\partial r)\,\lambda$ for a continuous shear profile $\vec{u} = u_z(r)\vec{e}_z$. This results in a characteristic acceleration timescale

$$t_{\rm acc} \simeq \frac{E}{dE/dt} \simeq \frac{\tau}{\langle \Delta E/E \rangle} \propto \frac{\tau}{\bar{u}^2} \propto \frac{1}{\lambda}, \tag{3}$$

scaling inversely with the particle mean free path λ or scattering time τ. While this makes shear flows also interesting for UHE cosmic-ray acceleration in the jets of AGNs [87], it typically requires some energetic seed injection for electron acceleration to proceed efficiently. In principle, this could be achieved by shock or classical 2nd order Fermi acceleration (for which $t_{\rm acc} \propto \lambda$) [82], or possibly, by kinetic-scale reconnection processes [88]. Phenomenologically, this could result in multi-component particle distributions, e.g., broken power-laws with changes in spectral indices different from a classical cooling break. A recent application shows that in the presence of a Kolmogorov-type $\lambda \propto \gamma^{1/3}$, the SED of the kpc-scale jet in Cen A can be successfully reproduced within a linear shear model for spine velocities of $v_j \simeq 0.7c$ and shear layer widths of $\Delta r \simeq 100$ pc [84]. In general, efficient shear acceleration requires relativistic flow speeds [89, 90] and this confines its applicability to astrophysical objects with fast outflows. There is currently a promising trend to incorporate particle acceleration and non-thermal emission recipes in large-scale MHD jet simulations, e.g. [91]. While such a hybrid approach is vital, it should be kept in mind that it still involves significant extrapolations (cf. Sec. 3.1.) that may need to be further explored. The prospects are good, though, for achieving further progress soon as several new observational facilities are coming online [15].

5. Conclusions

By providing new and often unexpected insights, multi-wavelengh and multi-messenger observations have become an indispensable tool for progress in many areas of astronomy. The field of AGNs, and in particular jetted AGNs, to which most extragalactic gamma-ray sources belong, is no exception in this regard [92]. In the present review, I have highlighted some of the developments that are of particular relevance for our understanding of the nature of these sources, and/or directly driven and inspired by gamma-ray observations, ranging from new observational findings to conceptual and methodological advances. I believe that we have seen true progress in our understanding of the physics of gamma-ray loud AGNs. As for jetted AGNs in general and for gamma-ray loud AGNs in particular: "The observational prospects for securing our understanding of AGN jets are bright." (Blandford et al., [15]). In particular, given available (from e.g. Fermi-LAT and the current IACTs, HESS, MAGIC and VERITAS to HAWC, LHAASO) and upcoming capabilities (CTA) at highest photon energies.

Acknowledgments

References

[1] P. Padovani, *On the two main classes of active galactic nuclei*, *Nature Astronomy* **1** (2017) 0194 [1707.08069].

[2] J. Biteau, E. Prandini, L. Costamante, M. Lemoine, P. Padovani, E. Pueschel et al., *Progress in unveiling extreme particle acceleration in persistent astrophysical jets*, *Nature Astronomy* **4** (2020) 124 [2001.09222].

[3] C.M. Urry and P. Padovani, *Unified Schemes for Radio-Loud Active Galactic Nuclei*, *PASP* **107** (1995) 803 [astro-ph/9506063].

[4] L. Costamante, *Blazars - an updated review*, in *Multifrequency Behaviour of High Energy Cosmic Sources - XIII. 3-8 June 2019. Palermo*, p. 35, Dec., 2020, DOI.

[5] C. Rulten, *Radio Galaxies at TeV Energies*, *Galaxies* **10** (2022) 61.

[6] S. Abdollahi, F. Acero, M. Ackermann, M. Ajello, W.B. Atwood, M. Axelsson et al., *Fermi Large Area Telescope Fourth Source Catalog*, *ApJS* **247** (2020) 33 [1902.10045].

[7] S. Abdollahi, F. Acero, L. Baldini, J. Ballet, D. Bastieri, R. Bellazzini et al., *Incremental Fermi Large Area Telescope Fourth Source Catalog*, *ApJS* **260** (2022) 53 [2201.11184].

[8] F. Rieger and A. Levinson, *Radio Galaxies at VHE Energies*, *Galaxies* **6** (2018) 116 [1810.05409].

[9] MAGIC Collaboration, V.A. Acciari, S. Ansoldi, L.A. Antonelli, A. Babić, B. Banerjee et al., *Study of the variable broadband emission of Markarian 501 during the most extreme Swift X-ray activity*, *A&A* **637** (2020) A86 [2001.07729].

[10] F. Aharonian, A.G. Akhperjanian, A.R. Bazer-Bachi, B. Behera, M. Beilicke, W. Benbow et al., *An Exceptional Very High Energy Gamma-Ray Flare of PKS 2155-304*, *ApJL* **664** (2007) L71 [0706.0797].

[11] S. Komossa, *Narrow-line Seyfert 1 Galaxies*, in *Revista Mexicana de Astronomia y Astrofisica Conference Series*, vol. 32 of *Revista Mexicana de Astronomia y Astrofisica Conference Series*, pp. 86–92, Apr., 2008, DOI [0710.3326].

[12] I. Varglund, E. Järvelä, A. Lähteenmäki, M. Berton, S. Ciroi and E. Congiu, *Jetted narrow-line Seyfert 1 galaxies breaking the jet paradigm – a comprehensive study of host galaxy morphologies*, *arXiv e-prints (A&A accepted)* (2022) arXiv:2209.09270 [2209.09270].

[13] F. D'Ammando, *Relativistic Jets in Gamma-Ray-Emitting Narrow-Line Seyfert 1 Galaxies*, *Galaxies* **7** (2019) 87 [1911.03500].

[14] L. Foschini, *Jetted Narrow-Line Seyfert 1 Galaxies & Co.: Where Do We Stand?*, *Universe* **6** (2020) 136 [2008.13383].

[15] R. Blandford, D. Meier and A. Readhead, *Relativistic Jets from Active Galactic Nuclei*, *ARA&A* **57** (2019) 467 [1812.06025].

[16] O. Porth, K. Chatterjee, R. Narayan, C.F. Gammie, Y. Mizuno, P. Anninos et al., *The Event Horizon General Relativistic Magnetohydrodynamic Code Comparison Project*, *ApJS* **243** (2019) 26 [1904.04923].

[17] K. Nishikawa, I. Duţan, C. Köhn and Y. Mizuno, *PIC methods in astrophysics: simulations of relativistic jets and kinetic physics in astrophysical systems*, *Living Reviews in Computational Astrophysics* **7** (2021) 1 [2008.02105].

[18] H. Ji and W. Daughton, *Phase diagram for magnetic reconnection in heliophysical, astrophysical, and laboratory plasmas*, *Physics of Plasmas* **18** (2011) 111207 [1109.0756].

[19] J. Kormendy and D. Richstone, *Inward Bound—The Search For Supermassive Black Holes In Galactic Nuclei*, *ARA&A* **33** (1995) 581.

[20] G. Katsoulakos, F.M. Rieger and B. Reville, *Constraining Cosmic-Ray Acceleration in the Magnetospheric Gaps of Sgr A**, *ApJL* **899** (2020) L7 [2007.12189].

[21] Event Horizon Telescope Collaboration, K. Akiyama, A. Alberdi, W. Alef, K. Asada, R. Azulay et al., *First M87 Event Horizon Telescope Results. I. The Shadow of the Supermassive Black Hole*, *ApJL* **875** (2019) L1 [1906.11238].

[22] R.D. Blandford and R.L. Znajek, *Electromagnetic extraction of energy from Kerr black holes.*, *MNRAS* **179** (1977) 433.

[23] Y. Mizuno, *GRMHD Simulations and Modeling for Jet Formation and Acceleration Region in AGNs*, *Universe* **8** (2022) 85 [2201.12608].

[24] B. Boccardi, T.P. Krichbaum, E. Ros and J.A. Zensus, *Radio observations of active galactic nuclei with mm-VLBI*, *A&ARv* **25** (2017) 4 [1711.07548].

[25] J.Y. Kim, T.P. Krichbaum, R.S. Lu, E. Ros, U. Bach, M. Bremer et al., *The limb-brightened jet of M87 down to the 7 Schwarzschild radii scale*, *A&A* **616** (2018) A188 [1805.02478].

[26] H. Sol, G. Pelletier and E. Asseo, *Two-flow model for extragalactic radio jets.*, *MNRAS* **237** (1989) 411.

[27] G. Ghisellini, F. Tavecchio and M. Chiaberge, *Structured jets in TeV BL Lac objects and radiogalaxies. Implications for the observed properties*, *A&A* **432** (2005) 401 [astro-ph/0406093].

[28] F. Mertens, A.P. Lobanov, R.C. Walker and P.E. Hardee, *Kinematics of the jet in M 87 on scales of 100-1000 Schwarzschild radii*, *A&A* **595** (2016) A54 [1608.05063].

[29] M. Janssen, H. Falcke, M. Kadler, E. Ros, M. Wielgus, K. Akiyama et al., *Event Horizon Telescope observations of the jet launching and collimation in Centaurus A*, *Nature Astronomy* **5** (2021) 1017 [2111.03356].

[30] G. Henri and L. Saugé, *The Bulk Lorentz Factor Crisis of TeV Blazars: Evidence for an Inhomogeneous Pileup Energy Distribution?*, *ApJ* **640** (2006) 185 [astro-ph/0511610].

[31] K. Hada, *Relativistic Jets from AGN Viewed at Highest Angular Resolution*, *Galaxies* **8** (2019) 1.

[32] Y.Y. Kovalev, A.B. Pushkarev, E.E. Nokhrina, A.V. Plavin, V.S. Beskin, A.V. Chernoglazov et al., *A transition from parabolic to conical shape as a common effect in nearby AGN jets*, *MNRAS* **495** (2020) 3576 [1907.01485].

[33] M. Nakamura, K. Asada, K. Hada, H.-Y. Pu, S. Noble, C. Tseng et al., *Parabolic Jets from the Spinning Black Hole in M87*, *ApJ* **868** (2018) 146 [1810.09963].

[34] J. Park, K. Hada, M. Kino, M. Nakamura, J. Hodgson, H. Ro et al., *Kinematics of the M87 Jet in the Collimation Zone: Gradual Acceleration and Velocity Stratification*, *ApJ* **887** (2019) 147 [1911.02279].

[35] V.S. Beskin and E.E. Nokhrina, *The effective acceleration of plasma outflow in the paraboloidal magnetic field*, *MNRAS* **367** (2006) 375.

[36] S.S. Komissarov, M.V. Barkov, N. Vlahakis and A. Königl, *Magnetic acceleration of relativistic active galactic nucleus jets*, *MNRAS* **380** (2007) 51 [astro-ph/0703146].

[37] M. Georganopoulos, E.S. Perlman and D. Kazanas, *Is the Core of M87 the Source of Its TeV Emission? Implications for Unified Schemes*, *ApJL* **634** (2005) L33 [astro-ph/0510783].

[38] E.T. Meyer, G. Fossati, M. Georganopoulos and M.L. Lister, *From the Blazar Sequence to the Blazar Envelope: Revisiting the Relativistic Jet Dichotomy in Radio-loud Active Galactic Nuclei*, *ApJ* **740** (2011) 98 [1107.5105].

[39] E.T. Meyer, M. Georganopoulos, W.B. Sparks, E. Perlman, R.P. van der Marel, J. Anderson et al., *A kiloparsec-scale internal shock collision in the jet of a nearby radio galaxy*, *Nature* **521** (2015) 495.

[40] A. Archer, W. Benbow, R. Bird, A. Brill, M. Buchovecky, J.H. Buckley et al., *VERITAS Discovery of VHE Emission from the Radio Galaxy 3C 264: A Multiwavelength Study*, *ApJ* **896** (2020) 41 [2005.03110].

[41] E. Lefa, F.M. Rieger and F. Aharonian, *Formation of Very Hard Gamma-Ray Spectra of Blazars in Leptonic Models*, *ApJ* **740** (2011) 64 [1106.4201].

[42] E. Lefa, F.A. Aharonian and F.M. Rieger, *"Leading Blob" Model in a Stochastic Acceleration Scenario: The Case of the 2009 Flare of Mkn 501*, *ApJL* **743** (2011) L19 [1108.4568].

[43] J. Biteau and M. Meyer, *Gamma-Ray Cosmology and Tests of Fundamental Physics*, *Galaxies* **10** (2022) 39 [2202.00523].

[44] F. Rieger, *Gamma-Ray Astrophysics in the Time Domain*, *Galaxies* **7** (2019) 28 [1901.10216].

[45] F.A. Aharonian, M.V. Barkov and D. Khangulyan, *Scenarios for Ultrafast Gamma-Ray Variability in AGN*, *ApJ* **841** (2017) 61 [1704.08148].

[46] F. Ait Benkhali, W. Hofmann, F.M. Rieger and N. Chakraborty, *Evaluating quasi-periodic variations in the γ-ray light curves of Fermi-LAT blazars*, *A&A* **634** (2020) A120 [1901.10246].

[47] P. Peñil, M. Ajello, S. Buson, A. Domínguez, J.R. Westernacher-Schneider and J. Zrake, *Evidence of Periodic Variability in Gamma-ray Emitting Blazars with Fermi-LAT*, *arXiv e-prints* (2022) arXiv:2211.01894 [2211.01894].

[48] E. Sobacchi, M.C. Sormani and A. Stamerra, *A model for periodic blazars*, *MNRAS* **465** (2017) 161 [1610.04709].

[49] M. Tavani, A. Cavaliere, P. Munar-Adrover and A. Argan, *The Blazar PG 1553+113 as a Binary System of Supermassive Black Holes*, *ApJ* **854** (2018) 11 [1801.03335].

[50] H. E. S. S. Collaboration, H. Abdalla, A. Abramowski, F. Aharonian, F. Ait Benkhali, A.G. Akhperjanian et al., *Characterizing the γ-ray long-term variability of PKS 2155-304 with H.E.S.S. and Fermi-LAT*, *A&A* **598** (2017) A39 [1610.03311].

[51] M. Polkas, M. Petropoulou, G. Vasilopoulos, A. Mastichiadis, C.M. Urry, P. Coppi et al., *A numerical study of long-term multiwavelength blazar variability*, *MNRAS* **505** (2021) 6103 [2105.07030].

[52] A. Dmytriiev, H. Sol and A. Zech, *Connecting steady emission and very high energy flaring states in blazars: the case of Mrk 421*, *MNRAS* **505** (2021) 2712 [2105.12480].

[53] P. Goldreich and W.H. Julian, *Pulsar Electrodynamics*, *ApJ* **157** (1969) 869.

[54] G. Katsoulakos and F.M. Rieger, *Gap-type Particle Acceleration in the Magnetospheres of Rotating Supermassive Black Holes*, *ApJ* **895** (2020) 99 [2005.05076].

[55] G. Katsoulakos and F.M. Rieger, *Magnetospheric Gamma-Ray Emission in Active Galactic Nuclei*, *ApJ* **852** (2018) 112 [1712.04203].

[56] A. Levinson and F. Rieger, *Variable TeV Emission as a Manifestation of Jet Formation in M87?*, *ApJ* **730** (2011) 123 [1011.5319].

[57] I. Contopoulos, *The immediate environment of an astrophysical black hole*, *MNRAS* **473** (2018) L146 [1711.00302].

[58] K. Hirotani, H.-Y. Pu, L.C.-C. Lin, H.-K. Chang, M. Inoue, A.K.H. Kong et al., *Lepton Acceleration in the Vicinity of the Event Horizon: High-energy and Very-high-energy Emissions from Rotating Black Holes with Various Masses*, *ApJ* **833** (2016) 142 [1610.07819].

[59] Event Horizon Telescope Collaboration, K. Akiyama, A. Alberdi, W. Alef, K. Asada, R. Azulay et al., *First M87 Event Horizon Telescope Results. V. Physical Origin of the Asymmetric Ring*, *ApJL* **875** (2019) L5 [1906.11242].

[60] F. Ait Benkhali, N. Chakraborty and F.M. Rieger, *Complex gamma-ray behavior of the radio galaxy M 87*, *A&A* **623** (2019) A2 [1802.03103].

[61] A.Y. Chen and Y. Yuan, *Physics of Pair Producing Gaps in Black Hole Magnetospheres. II. General Relativity*, *ApJ* **895** (2020) 121 [1908.06919].

[62] B. Crinquand, B. Cerutti, A. Philippov, K. Parfrey and G. Dubus, *Multidimensional Simulations of Ergospheric Pair Discharges around Black Holes*, *Phys Rev Lett.* **124** (2020) 145101 [2003.03548].

[63] S. Kisaka, A. Levinson and K. Toma, *Comprehensive Analysis of Magnetospheric Gaps around Kerr Black Holes Using 1D GRPIC Simulations*, *ApJ* **902** (2020) 80 [2007.02838].

[64] S. Kisaka, A. Levinson, K. Toma and I. Niv, *The Response of Black Hole Spark Gaps to External Changes: A Production Mechanism of Rapid TeV Flares?*, *ApJ* **924** (2022) 28 [2108.02971].

[65] M. Cerruti, *Leptonic and Hadronic Radiative Processes in Supermassive-Black-Hole Jets*, *Galaxies* **8** (2020) 72 [2012.13302].

[66] H. Sol and A. Zech, *Blazars at Very High Energies: Emission Modelling*, *Galaxies* **10** (2022) 105 [2211.03580].

[67] A. Zech and M. Lemoine, *Electron-proton co-acceleration on relativistic shocks in extreme-TeV blazars*, *A&A* **654** (2021) A96 [2108.12271].

[68] P. Crumley, D. Caprioli, S. Markoff and A. Spitkovsky, *Kinetic simulations of mildly relativistic shocks - I. Particle acceleration in high Mach number shocks*, *MNRAS* **485** (2019) 5105 [1809.10809].

[69] L. Sironi, A. Spitkovsky and J. Arons, *The Maximum Energy of Accelerated Particles in Relativistic Collisionless Shocks*, *ApJ* **771** (2013) 54 [1301.5333].

[70] A. Vanthieghem, M. Lemoine, I. Plotnikov, A. Grassi, M. Grech, L. Gremillet et al., *Physics and Phenomenology of Weakly Magnetized, Relativistic Astrophysical Shock Waves*, *Galaxies* **8** (2020) 33 [2002.01141].

[71] S.K. Jagan, S. Sahayanathan, F.M. Rieger and C.D. Ravikumar, *Convex X-ray spectra of PKS 2155-304 and constraints on the minimum electron energy*, *MNRAS* **506** (2021) 3996 [2107.04534].

[72] I. Liodakis, D. Blinov, S.B. Potter and F.M. Rieger, *Constraints on magnetic field and particle content in blazar jets through optical circular polarization*, *MNRAS* **509** (2022) L21 [2110.11434].

[73] G.E. Romero, *The content of astrophysical jets*, *Astronomische Nachrichten* **342** (2021) 727 [2106.14346].

[74] F. Tavecchio, A. Costa and A. Sciaccaluga, *Extreme blazars: the result of unstable recollimated jets?*, *MNRAS* **517** (2022) L16 [2207.12766].

[75] D.E. Harris and H. Krawczynski, *X-Ray Emission from Extragalactic Jets*, *ARA&A* **44** (2006) 463 [astro-ph/0607228].

[76] M. Georganopoulos, E. Meyer and E. Perlman, *Recent Progress in Understanding the Large Scale Jets of Powerful Quasars*, *Galaxies* **4** (2016) 65.

[77] P. Breiding, E.T. Meyer, M. Georganopoulos, M.E. Keenan, N.S. DeNigris and J. Hewitt, *Fermi Non-detections of Four X-Ray Jet Sources and Implications for the IC/CMB Mechanism*, *ApJ* **849** (2017) 95 [1710.04250].

[78] P. Breiding, E.T. Meyer, M. Georganopoulos, K. Reddy, K.E. Kollmann and A. Roychowdhury, *A multiwavelength study of multiple spectral component jets in AGN: testing the IC/CMB model for the large-scale-jet X-ray emission*, *MNRAS* **518** (2023) 3222 [2210.13104].

[79] X.-N. Sun, R.-Z. Yang, F.M. Rieger, R.-Y. Liu and F. Aharonian, *Energy distribution of relativistic electrons in the kiloparsec scale jet of M 87 with Chandra*, *A&A* **612** (2018) A106 [1712.06390].

[80] H. E. S. S. Collaboration, H. Abdalla, R. Adam, F. Aharonian, F. Ait Benkhali, E.O. Angüner et al., *Resolving acceleration to very high energies along the jet of Centaurus A*, *Nature* **582** (2020) 356 [2007.04823].

[81] H. E. S. S. Collaboration, H. Abdalla, A. Abramowski, F. Aharonian, F. Ait Benkhali, E.O. Angüner et al., *The γ-ray spectrum of the core of Centaurus A as observed with H.E.S.S. and Fermi-LAT*, *A&A* **619** (2018) A71 [1807.07375].

[82] R.-Y. Liu, F.M. Rieger and F.A. Aharonian, *Particle Acceleration in Mildly Relativistic Shearing Flows: The Interplay of Systematic and Stochastic Effects, and the Origin of the Extended High-energy Emission in AGN Jets*, *ApJ* **842** (2017) 39 [1706.01054].

[83] F. Tavecchio, *Constraining the shear acceleration model for the X-ray emission of large-scale extragalactic jets*, *MNRAS* **501** (2021) 6199 [2011.03264].

[84] J.-S. Wang, B. Reville, R.-Y. Liu, F.M. Rieger and F.A. Aharonian, *Particle acceleration in shearing flows: the case for large-scale jets*, *MNRAS* **505** (2021) 1334 [2105.08600].

[85] J.-S. Wang, B. Reville, Y. Mizuno, F.M. Rieger and F.A. Aharonian, *Particle acceleration in shearing flows: the self-generation of turbulent spine-sheath structures in relativistic MHD jet simulations*, *arXiv e-prints* (2022) arXiv:2212.03226 [2212.03226].

[86] F.M. Rieger, *An Introduction to Particle Acceleration in Shearing Flows*, *Galaxies* **7** (2019) 78 [1909.07237].

[87] F.M. Rieger, *Active Galactic Nuclei as Potential Sources of Ultra-High Energy Cosmic Rays*, *Universe* **8** (2022) 607 [2211.12202].

[88] L. Sironi, M.E. Rowan and R. Narayan, *Reconnection-driven Particle Acceleration in Relativistic Shear Flows*, *ApJL* **907** (2021) L44 [2009.11877].

[89] G.M. Webb, A.F. Barghouty, Q. Hu and J.A. le Roux, *Particle Acceleration Due to Cosmic-ray Viscosity and Fluid Shear in Astrophysical Jets*, *ApJ* **855** (2018) 31.

[90] F.M. Rieger and P. Duffy, *Particle Acceleration in Relativistic Shearing Flows: Energy Spectrum*, *ApJ* **933** (2022) 149 [2206.13098].

[91] D. Mukherjee, G. Bodo, P. Rossi, A. Mignone and B. Vaidya, *Simulating the dynamics and synchrotron emission from relativistic jets - II. Evolution of non-thermal electrons*, *MNRAS* **505** (2021) 2267 [2105.02836].

[92] M. Böttcher, *Progress in Multi-wavelength and Multi-Messenger Observations of Blazars and Theoretical Challenges*, *Galaxies* **7** (2019) 20 [1901.04178].